Comparison of Guaranteed State Estimators for Linear Time-Invariant Systems ⋆

Matthias Althoff [a] and Jagat Jyoti Rath [b]

[a] *Department of Informatics, Technische Universität München, 80333 München, Germany.*

[b] *Department of Mechanical and Aero-Space Engineering, Institute of Infrastructure Technology Research and Management,Ahmedabad - 380026 India.*

Abstract

Guaranteed state estimation computes the set of possible states of dynamical systems given the bounds of model uncertainties, disturbances, and noises. For the first time, we evaluate and compare a broad class of guaranteed state estimators for linear time-invariant systems regarding scalability, accuracy, and real-time applicability. In particular, we consider strip-based observers, set-propagation observers, and interval observers. The performance of most guaranteed state estimators is significantly affected by the chosen set representation. Zonotopes have emerged as a popular set representation since important operations such as linear maps and Minkowski sum can be computed exactly and efficiently. Furthermore, we provide comparisons with ellipsoids and constrained zonotopes as set representations. The comparison is conducted on various models for state estimation of autonomous vehicles.

Key words: Guaranteed state estimation, set-based observers, strip-based observers, set-propagation observers, interval observers, zonotopes, ellipsoids, constrained zonotopes, comparison, linear time-invariant systems.

1 Introduction

Systems are becoming increasingly autonomous, such as automated road vehicles, surgical robots, automatic operation of smart grids, and collaborative human-robot manufacturing. Hence, they are increasingly safety-critical and/or operation-critical [54], [47]. Controlling these systems requires state observers, because the full system state is typically not measured due to, e.g., a lack of measuring devices, packaging problems, or just economic reasons. While estimating the most likely state is sufficient for non-critical applications, critical systems require the entire set of possible states from guaranteed state estimation [1, 10, 11, 18, 22, 61]. The set of possible states can be used to rigorously predict future behaviors [5, 25], perform robust control [40, 60], perform conformance checking [58], or apply robust fault detection [75]. We consider rigorous state estimation of linear time-invariant systems, which can also be used to observe nonlinear systems when using conservative linearization techniques, see, e.g., [8, 20].

⋆ Corresponding author: J. J. Rath, Email: jagatjyoti.rath@gmail.com

Email addresses: althoff@tum.de (Matthias Althoff), jagat.rath@iitram.ac.in (Jagat Jyoti Rath).

Types of Set-Based Observers: In essence, three types of set-based observers have been developed in the last decades: strip-based observers, set-propagation observers, and interval observers. Strip-based observers propagate the set of possible states forward using reachability analysis [3], followed by intersecting it with strips of possible states from measurements; see, e.g., [1, 11, 18, 61]. Set-propagation observers do not require intersecting sets and propagate sets based on the joint use of reachability analysis and the concept of a Luenberger observer [22, 50]. Finally, interval observers consist of two separate observers that provide an upper and lower bound so that state variables are bounded within intervals [24, 29, 46, 55, 77]. We would like to mention that historically, strip-based observers are often also referred to as set membership observers; however, in principle all guaranteed observers compute set memberships. Also, some papers bound their states by intervals and refer to them as interval observers; however, we prefer to categorize the observers algorithmically rather than based on the set representation.

Typical Set Representations: One of the barriers to wide-spread use of guaranteed state estimation is their higher computational cost compared to classical observers. Choosing an appropriate set representation

is a key design choice. For instance, by modeling sets as the convex hull of vertices, an axis-aligned box in $\mathbb{R}^n$ would already have 2^n vertices so that just storing a single set is infeasible in high-dimensional spaces. Besides the representation size, it is important that relevant operations can be efficiently computed or over-approximated. Guaranteed state estimation requires linear maps and Minkowski sum. For strip-based approaches, one additionally requires intersection. The importance of set representations led to exploring ellipsoids [10,11,17,61], zonotopes [1,22,50,52], constrained zonotopes [56, 57, 62], and polytopes [32]. However, ellipsoids are not closed under Minkowski sum and intersection, requiring to compute overly large over-approximations [23,28,48]. To obtain tighter sets, polytopes have been suggested at the expense of large computational costs, e.g., computing the Minkowski sum of two polytopes for $n = 20$ is computationally infeasible. To reduce computation time, parallelotopes as a special class of polytopes are discussed in [18, 32]. However, paralellotopes are also not closed under Minkowski sum, resulting in conservative results. While constrained zonotopes can represent any polytope and perform Minkowski sums more efficiently, it requires linear programming to compute the ranges of values in a given direction. To obtain a good balance of accuracy and computational costs, zonotopes [3, 33] are widely used in recent works since they are closed under Minkowski sum and linear maps. Due to the recent popularity of zonotopic state observers, we focus on this set representation subsequently.

Zonotopic Strip-Based Observers: Although zonotopes are not closed under intersection like ellipsoids, intersection of zonotopes can be efficiently over-approximated. Previous works mostly differ in how the intersection is over-approximated: a) singular value decomposition is used in [19], which is computationally efficient, but does not optimize a particular performance metric; b) segment minimization and volume minimization [1] overcome limitations of the singular-value-decomposition approach. However, segment minimization leads to conservative results when handling uncertainties across multiple dimensions [35, 38], while volume minimization is computationally expensive [35]. Combining the merits of both approaches, a novel P-radius minimization technique provides a good ratio of accuracy and computation costs [35, 36, 38, 39]. Since the previously-mentioned designs lead to conservative results for high-dimensional systems, a novel P-radius-based estimation is proposed in [37] for uncertain multi-output linear systems considering all measurements simultaneously. The continuous improvement of zonotopic strip-based observers led to several applications for parameter estimation and fault diagnosis, among others [12,51].

Zonotopic Set-Propagation and Interval Observers: Let us subsequently survey zonotopic set-propagation observers. P-radius minimization has also been applied to set-propagation observers [64, 71, 73]. Similarly, in [22], a special type of set-propagation observer is proposed to minimize the Frobenius norm of the estimation error while ensuring robustness and making explicit links with Kalman filters. Zonotopic set-propagation observers have also been applied to fault detection [13,21,69,70], parameter estimation [66], and feedback control problems [74]. To avoid the wrapping effect of zonotopic observers, an H-infinity interval observers is presented in [65].

Contributions: In summary, many aspects of zonotopic state observer design, such as accuracy, scalability, and computational costs are not yet compared in detail. A comparative analysis between zonotopic strip-based and set-propagation observers for a single-output system was presented in [49] [1] . Extending this work, a comparison analysis for fault detection using zonotopic strip-based and set-propagation observers is performed in [50] [1] . For the first time, we present a comprehensive comparison of different zonotopic observers for linear time-invariant systems with the following features:

- Comparison between strip-based observers, set-propagation observers, and interval observers.
- Comparison between observers using different minimization techniques, such as volume minimization, F-radius minimization, P-radius minimization, and H-infinity minimization.
- Comparison between zonotopes, constrained zonotopes, and ellipsoids as set representations.
- Consideration of single-output and multi-output estimation.
- Scalability analysis and assessment of real-time capabilities.
- Performance analysis with respect to different parameter settings, such as the used zonotope order.

For performing the comparison, we consider vehicle-side-slip estimation for road vehicles [68].

2 Preliminaries

Let us first give a brief introduction to strip-based observers, set-propagation observers, and interval observers for linear time-invariant systems.

2.1 Set Representations

Before we introduce specific sets, let us first introduce the following set operations for $\mathcal{S}_1, \mathcal{S}_2 \subset \mathbb{R}^n$:

- *Linear map*: $M\mathcal{S}_1 = \{Ms_1 \mid s_1 \in \mathcal{S}_1\}, M \in \mathbb{R}^{n\times n}$.

[1] That work refers to strip-based observers as set membership observers and to set-propagation observers as interval observers.

- *Minkowski sum*: $\mathcal{S}_1 \oplus \mathcal{S}_2 = \{s_1 + s_2 \mid s_1 \in \mathcal{S}_1, s_2 \in \mathcal{S}_2\}$.

One of the simplest set representations are intervals: $[\underline{x}, \overline{x}] = \{x \in \mathbb{R} \mid \underline{x} \leq x \leq \overline{x}\}$. An axis-aligned box is an interval vector $[\ [\underline{x}_1, \overline{x}_1], [\underline{x}_2, \overline{x}_2], ...[\underline{x}_n, \overline{x}_n]\ ]^T$. We define the unit interval as $\mathcal{B} = [-1, 1]$ and the unit box in $\mathbb{R}^n$ as $\mathcal{B}^n$. A more general set representation than intervals are polyhedra, which can be defined as the intersection of m half-spaces (H-representation) [17, eq. 3.20]:

$$\mathcal{P} = \Big\{ x \in \mathbb{R}^n \Big| Dx \leq d \Big\}, \tag{1}$$

where $D \in \mathbb{R}^{m \times n}$ and $d \in \mathbb{R}^m$. A bounded polyhedral set is called a polytope. A class of centrally-symmetric polytopes are called zonotopes and are represented as

$$\mathcal{Z} = c \oplus G\mathcal{B}^r,$$

where $c \in \mathbb{R}^n$ is the center, $G \in \mathbb{R}^{n \times r}$ is a matrix representing the generators, and r/n is the order of the zonotope [3, Sec. 2.1] [2] . When adding a linear constraint $A\xi = b$ to zonotopes, where $A \in \mathbb{R}^{n_c \times r}$, $b \in \mathbb{R}^{n_c}$, and ξ is the vector that is mapped by the generator matrix, one obtains a constrained zonotope [62, Def. 3]:

$$\mathcal{CZ} = \{c + G\xi | \xi \in \mathcal{B}^r, A\xi = b\}.$$

Finally, we present ellipsoids, which are defined by a symmetric positive definite matrix $H = H^T \succ 0$, and the center $c \in \mathbb{R}^n$ as [17, eq. 3.33]

$$\mathcal{E}(H, c) = \Big\{ x \in \mathbb{R}^n \ \Big| \ (x - c)^T H (x - c) \leq 1 \Big\}.$$

2.2 Cost Functions

To minimize the size of the estimated sets, we define the following costs of a zonotope $\mathcal{Z} = c \oplus G\mathcal{B}^r$:

- **Volume:** The volume of a zonotope (see [1, Sec. 6.2]).
- **F_P-radius:** Given a symmetric weighting matrix $P \in \mathbb{R}^{n \times n}$, $P = P^T \succ 0$, the F_P-radius is the weighted Frobenius norm of G [22, Def. 2]:

  $$F_P = \|G\|_{F,P} = \sqrt{\text{trace}(G^T P G)}.$$

  When the weighting matrix is the identity, i.e., $P = I \in \mathbb{R}^{n \times n}$, we say that the F-radius instead of the F_P radius is obtained.
- **P-radius:** For a positive definite symmetric matrix $P = P^T \succ 0$, the P-radius [38, Sec. 2] is

  $$\Theta = \max_{z \in \mathcal{Z}} (\|z - c\|_P^2) = \max_{z \in \mathcal{Z}} ((z - c)^T P (z - c)).$$

[2] Please note that, in some other works, the order of a zonotope is defined as r, see, e.g., [1, Sec. 4.1], [15, Def. 6].

2.3 Problem Statement

We consider discrete-time, linear, time-invariant disturbed systems, with state $x_k \in \mathbb{R}^n$, input $u_k \in \mathbb{R}^{n_u}$, output $y_k \in \mathbb{R}^{n_y}$, disturbance $w_k \in \mathbb{R}^{n_w}$, and sensor noise $v_k \in \mathbb{R}^{n_v}$ at step k:

$$\begin{aligned} x_{k+1} &= Ax_k + Bu_k + w_k, \\ y_k &= Cx_k + v_k, \end{aligned} \tag{2}$$

where A, B, and C are matrices of proper dimensions. It is assumed that the system is observable and that the disturbance is bounded by the zonotopes $\mathcal{W} = E\mathcal{B}^{n_w}$ and the noise is bounded by the set $\mathcal{V} = F\mathcal{B}^{n_v}$. Please note that other works use $\tilde{E}\tilde{w}_k$ and $\tilde{F}\tilde{v}_k$ instead of w_k and v_k in (2), however, this is not a more general case since one can simply choose $\mathcal{W} = \tilde{E}\tilde{\mathcal{W}}$ and $\mathcal{V} = \tilde{F}\tilde{\mathcal{V}}$. A possible way to automatically find proper sets $\mathcal{W}$ and $\mathcal{V}$ is through conformance checking, see, e.g., [30, 41, 59]. For a given state x_k, input u_k, and disturbance w_k, let us denote the next state of (2) by $\chi(x_k, u_k, w_k)$.

Our objective is to find the sets of possible states at time step k, which we define inductively starting with the initial set $\mathcal{S}_0 \subset \mathbb{R}^n$:

$$\begin{aligned} \mathcal{S}_k = \Big\{ x_k = \chi\Big(x_{k-1}, u_{k-1}, w_{k-1}\Big) \Big| x_{k-1} \in \mathcal{S}_{k-1}, \\ w_{k-1} \in \mathcal{W}, v_k \in \mathcal{V}, y_k = Cx_k + v_k \Big\}. \end{aligned} \tag{3}$$

We aim at computing an over-approximation of $\mathcal{S}_k$ that minimizes the previously-presented cost functions. This goal is pursued differently for the strip-based, set-propagation, and interval observers presented subsequently.

2.4 Strip-Based Observers

Strip-based observers first propagate the possible set of states according to the system dynamics, which is intersected by the set of possible states due to the current measurement:

(1) *Prediction*: By evaluating (2) in a set-based fashion, one obtains the next set of possible states [38, Def. 2]:
$$\mathcal{S}^p = A\mathcal{S}_{k-1} \oplus Bu_{k-1} \oplus \mathcal{W}.$$
(2) *Measurement update*: Due to the linear measurement function in (2), the possible states from the measurement of the j^{th} output signal $y_{k,j}$ at time

step k are bounded by a strip of width σ_j [1, Property 2]:

$$\hat{\mathcal{S}}_j = \left\{ x \in \mathbb{R}^n \middle| |C_j x - y_{k,j}| \leq \sigma_j \right\}, \quad (4)$$

where C_j is the j^{th} row of the measurement matrix C in (2) and σ is the symmetric bound of the box enclosing the sensor noise: $[-\sigma, \sigma] = \text{BOX}(\mathcal{V})$. The entire measurement set $\mathcal{S}_y$ is computed by over-approximating the intersection of all strips:

$$\hat{\mathcal{S}} \subseteq \hat{\mathcal{S}}_1 \cap \hat{\mathcal{S}}_2 \ldots \cap \hat{\mathcal{S}}_{n_y}. \quad (5)$$

(3) *Correction*: The set consistent with the propagated set $\mathcal{S}^p$ and the measurement set $\hat{\mathcal{S}}$ is simply obtained by intersection, which is often over-approximated for computational efficiency [1, Sec.3]:

$$\mathcal{S}_k \supseteq \mathcal{S}^p \cap \hat{\mathcal{S}}. \quad (6)$$

Next, we present set-propagation approaches, which do not require to perform intersections.

2.5 Set-Propagation Observers

A disadvantage of the strip-based approach is that efficient set representations, such as ellipsoids and zonotopes, are not closed under intersection. Set-propagation approaches eliminate this problem, which are typically based on the update equation of a Luenberger observer:

$$\hat{x}_{k+1} = A\hat{x}_k + Bu_k + w_k + L(y_k - C\hat{x}_k - v_k), \quad (7)$$

where $\hat{x}_{k+1}$ is the estimated state at step $k+1$. The observer gain L is designed so that the estimated state quickly converges to the true state. A simple and direct way to obtain guaranteed state estimation is to evaluate (7) in a set-based fashion [22, Sec. 4.1]:

$$\mathcal{S}_{k+1} = (A - LC)\mathcal{S}_k \oplus Bu_k \oplus Ly_k \oplus (-L)\mathcal{V} \oplus \mathcal{W}. \quad (8)$$

It is fairly easy to see that (8) is over-approximative if $\hat{x}_0 \in \mathcal{S}_0$ and $\mathcal{V}$ as well as $\mathcal{W}$ contain the origin: The true solution is $x_{k+1} = Ax_k + Bu_k + w_k$ according to (7). Since $\mathcal{V}$ and $\mathcal{W}$ contain the origin, their set-based evaluation only inflates the true evolution of the state so that the state inclusion holds for any L. The matrix gain L can thus be used to optimize the estimation accuracy based on cost functions from Sec. 2.2, either offline (constant gain) or online (time-varying gain).

2.6 Interval Observers

Yet another possibility to avoid intersections is to bound the state by two observers when exploiting monotonicity of the system dynamics [65, Sec. VI]. Since often the dynamics is not monotone, a new method is presented in [65, Alg. 1], which is proven to be at least as good as the classical interval observers exploiting monotonicity. The proposed approach in Alg. 1 is based on (8) and avoids the wrapping effect by re-arranging the computation of (8) and using the box operator analogously to [27].

Algorithm 1 Interval observer from [65, Alg. 1].

Input: input sequence u_k, output sequence y_k
Output: Sequence of state bounds $\underline{x}_k$, $\overline{x}_k$.

$\hat{x}_0 \leftarrow \text{CENTER}(\mathcal{X}_0)$, $\quad \mathcal{D}_0 \leftarrow \mathcal{W} \oplus (-L)\mathcal{V}$
$\mathcal{S}_{x,0} \leftarrow \mathcal{X}_0$, $\quad \mathcal{S}_{wv,0} \leftarrow \mathbf{0}$
for all $k \geq 0$ **do**
  $[\underline{e}_k, \overline{e}_k] = \text{BOX}(\mathcal{S}_{x,k}) \oplus \mathcal{S}_{wv,k}$
  $[\underline{x}_k, \overline{x}_k] = \hat{x}_k + [\underline{e}_k, \overline{e}_k]$
  $\hat{x}_{k+1} = A\hat{x}_k + Bu_k + L(y_k - C\hat{x}_k)$
  $\mathcal{S}_{x,k+1} = (A - LC)\mathcal{S}_{x,k}$
  $\mathcal{S}_{wv,k+1} = \mathcal{S}_{wv,k} \oplus \text{BOX}(\mathcal{D}_k)$
  $\mathcal{D}_{k+1} = (A - LC)\mathcal{D}_k$
end for

2.7 Summary

In [71, Sec. 5] it has been shown that there exists a parameterization for the set-propagation approach and the strip-based approach such that both approaches produce exactly the same result. However, no general procedure is known that converts one approach into the other one. Given a state-of-the art parameterization of each method, it is unclear which method performs better in which application. We try to shed some light into this question in this paper. Next, we present concrete realizations of the presented observer types when using zonotopes as a set representation.

Strip-based observers can only finish their computation of the estimated set $\mathcal{S}_k$ after receiving the measurement y_k. As a consequence, the estimated set $\mathcal{S}_k$ arrives with a delay. This problem does not occur when using set-propagation observers and interval observers, which obtain $\mathcal{S}_k$ before time step k when the implementation is real-time capable. To retain formal correctness, it would be required for strip-based observers to additionally compute a one-step prediction of the set of states and use this set as the set of initial states as shown in [60, Sec. III]. Since some practitioners may want to ignore the delayed computation (e.g. in a fault-detection algorithm), we list the computation times in Tab. 3 without the additional prediction step, but indicate that these algorithms are not necessarily ready to be used for control. Our experiments have shown that adding a second prediction would roughly increase the computation in Tab. 3 by 0.1 ms.

3 Zonotopic Observers

As shown in Sec. 2, guaranteed state estimation mainly requires linear maps, Minkowski sums, and intersections.

While constrained zonotopes are closed under these operations, they require solving linear programs to obtain ranges of state intervals. A comparison between the remaining set representations, namely ellipsoids, zonotopes, and polytopes, is shown in Tab. 1 for the mentioned operations. We assume that the resulting sets in Tab. 1 are not reduced, e.g., redundant inner points of a V-polytope are not removed.

Table 1
Comparison of set representations for unreduced results when the linear map $M\,\mathcal{S}$ is performed with a square matrix M of full rank (✗: not closed under set operation).

Set Representation	**Linear Map**	**Mink. Sum**	**Intersection**
H-Polytopes (spanned by n generators)	$\mathcal{O}(n^3)$ † [14, Tab. 1]	$\mathcal{O}(2^n)$ [14, Tab. 1]	$\mathcal{O}(1)$ eq. (1)
V-Polytopes (spanned by n generators)	$\mathcal{O}(n^2 2^n)$ [14, Tab. 1]	$\mathcal{O}(n 2^{2n})$ [14, Tab. 1]	super-polynomial [3] [16, Ch. 6.1]
Ellipsoids	$\mathcal{O}(n^3)$ [34, Sec. 2.2.1]	✗	✗
Zonotopes (n generators)	$\mathcal{O}(n^3)$ [6, Tab. I]	$\mathcal{O}(n)$ [6, Tab. I]	✗

It can be seen from Tab. 1 that zonotopes provide higher accuracy compared to using ellipsoids and lower computational complexity compared to polytopes. Thus, we will only present zonotopic observers in this section; we assume that the set of initial states $\mathcal{X}_0$, the set of disturbances $\mathcal{W}$, and the set of noises $\mathcal{V}$ are bounded by zonotopes. If these sets are not zonotopes, one could over-approximate them by zonotopes.

3.1 Strip-Based Observers

Strip-based observers using zonotopes only differ in the way the intersection in (5) and (6) is over-approximated after obtaining the predicted zonotope $\mathcal{S}^p = c^p \oplus G^p \mathcal{B}^r$. A graphical representation of the intersection methods is presented in Fig. 1, which are briefly introduced subsequently.

Intersection method I: By considering the multi-output system (2) as n_y separate single-output systems, the intersection of the predicted zonotope $\mathcal{S}^p$ and the first strip $\hat{\mathcal{S}}_1$ in (4) can be over-approximated by a family of zonotopes parameterized by $\lambda^1 \in \mathbb{R}^n$ [1, Sec. 6] [38, Sec. 4]:

$$\begin{aligned}\hat{\mathcal{Z}}_1(\lambda^1) =&(I - \lambda^1 C_1)c^p + \lambda^1 y_{k,1} \oplus \\ &[(I - \lambda^1 C_1)G^p,\ \lambda^1 \sigma_1]\mathcal{B}^{r+1},\end{aligned}$$

where I is the identity matrix of proper dimension. The resulting zonotope is then intersected with the strip $\hat{\mathcal{S}}_2$ corresponding to the second output. This procedure is repeated until the last measurement to obtain the final estimated set from $\hat{\mathcal{Z}}_{n_y-1} = \hat{c} \oplus \hat{G}\mathcal{B}^{r+n_y-1}$ [38, Sec. 4]:

$$\begin{aligned}\mathcal{S}_k = \hat{\mathcal{Z}}_{n_y}(\lambda^{n_y}) =&(I - \lambda^{n_y} C_{n_y})\hat{c} + \lambda^{n_y} y_{k,n_y} \oplus \\ &[(I - \lambda^{n_y} C_{n_y})\hat{G},\ \lambda^{n_y} \sigma_{n_y}]\mathcal{B}^{r+n_y}.\end{aligned}$$

For a compact notation, we store all λ^i in $\Lambda = [\lambda^1, \ldots, \lambda^{n_y}] \in \mathbb{R}^{n \times n_y}$.

Intersection method II: This method (see [37, Sec. IV]) first computes the exact polytope of the intersections in (5):

$$\hat{\mathcal{S}} = \Big\{ x \in \mathbb{R}^n \Big| |Cx - y_k| \leq \sigma \Big\}.$$

The intersection with the propagated zonotope in (6) is over-approximated by a zonotope parameterized by Λ [37, Sec. IV]:

$$\begin{aligned}\mathcal{S}_k(\Lambda) =&(I - \Lambda C)c^p + \Lambda y_k \\ &\oplus [(I - \Lambda C)G^p,\ \Lambda\ \mathrm{diag}(\sigma)]\mathcal{B}^{r+n_y},\end{aligned}$$

where diag() returns a diagonal matrix.

Intersection method III: The family of zonotopes over-approximating the intersection of $\mathcal{S}^p$ with the first strip according to [15, Sec. III.B] is $\hat{\mathcal{Z}}_1(j) = c(j) \oplus G(j)\mathcal{B}^r$ for any integer j, $0 \leq j \leq r$ using the j^{th} column g^j of G^p, where

$$c(j) = \begin{cases} c^p + \frac{y_{k,1} - C_1 c^p}{C_1 g^j} g^j;\ \text{if } 1 \leq j \leq r, C_1 g^j \neq 0, \\ c^p;\ \text{otherwise,} \end{cases}$$

$$G(j) = \begin{cases} [\tilde{G}_1\ \tilde{G}_2 ... \tilde{G}_r];\ \text{if } 1 \leq j \leq r, C_1 g^j \neq 0, \\ G^p;\ \text{otherwise,} \end{cases}$$

$$\tilde{G}_o = \begin{cases} g^o - \frac{C_1 g^o}{C_1 g^j};\ \text{if } o \neq j, \\ \frac{\sigma_1}{C_1 g^j} g^j;\ \text{if } o = j. \end{cases}$$

Similar to parameterization method I, this zonotope is then intersected with the next strips n_y times until the final estimated zonotopic set $\mathcal{S}_k$ is computed.

To design Λ for intersection methods I and II, and to obtain the optimal bounding zonotope for method III, different cost functions and convex optimization techniques are employed as shown in Tab. 2. For P-radius minimization, the design parameters in Λ can be obtained by solving the respective optimization problems as bilinear matrix inequalities. For ease of design, the bi-

[3] Intersection has to be performed by facet and vertex enumeration.

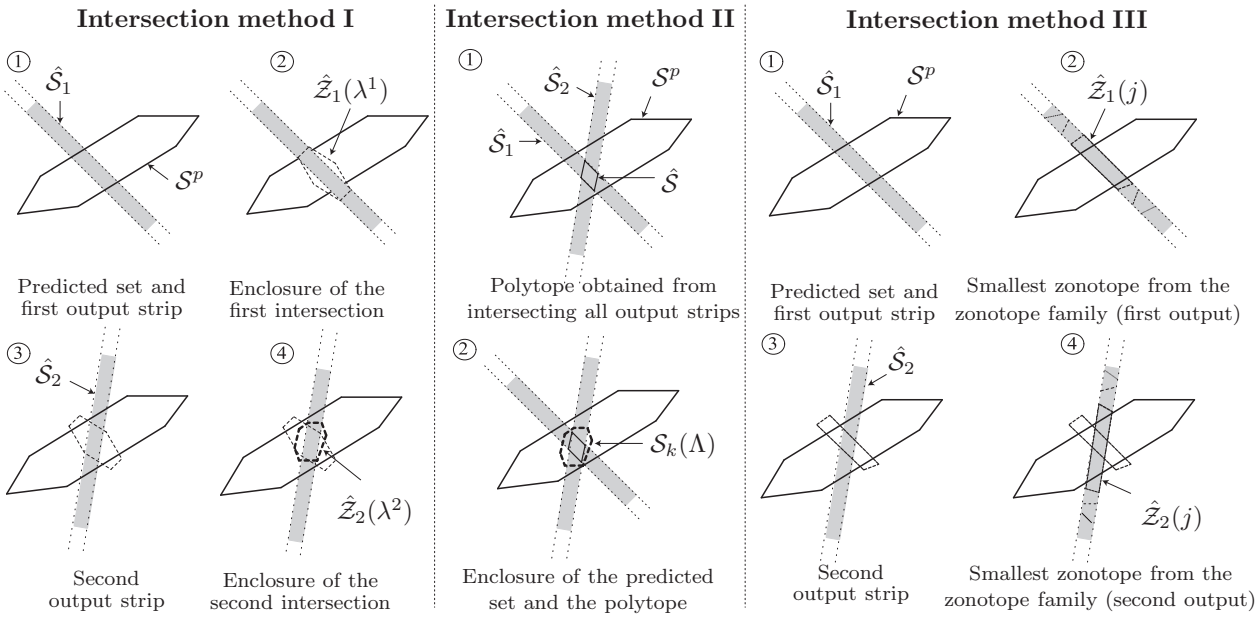

Fig. 1. Graphical representation of all intersection methods for the multi-output case

linear matrix inequalities can also be solved as a group of linear matrix inequalities by performing a line search or using bisection algorithms [37,38]. Such an approach reduces the number of decision variables and thus reduces the complexity of solving the linear matrix inequalities.

Irrespective of the parameterization method, all volume minimization and F-radius techniques involve solving an optimization problem in each step during real-time operation. In contrast, Λ is pre-computed before real-time operation for all P-radius techniques.

Table 2
Combinations of intersection methods and cost functions.

Intersection	**Cost function**		
	volume	**F-radius**	**P-radius**
I	VolMin-A [1]	FRad-A [1]	PRad-A [38]
II		FRad-B [71]	PRad-B [37], PRad-C-I [71], PRad-C-II [67], PRad-D [72]
III	VolMin-B [15]		

3.2 Set-Propagation Observers

We now discuss various techniques for optimizing the observer gain L of (8) for set-propagation observers.

F-radius minimization (FRad-C): Using an analogous procedure as for the Kalman filter, the optimal gain L to minimize the F-radius of $\mathcal{S}_k = c \oplus G\mathcal{B}^r$ is [22, Sec. 4.3]:

$$L = AGG^TC^T[CGG^TC^T + FF^T]^{-1}.$$

P-radius minimization (PRad-E): The observer gain L minimizing the P-radius of $\mathcal{S}_k$ is [73, eq. 17]:

$$L = P^{*-1}Q, \quad P^* = \operatorname{argmax}(\operatorname{trace}(P))$$

subject to

$$\begin{bmatrix} -\beta P & 0 & 0 & A^TP - C^TQ^T \\ \star & -E^TE & 0 & E^TP \\ \star & \star & -F^TF & F^TQ^T \\ \star & \star & \star & -P \end{bmatrix} \prec 0,$$

where $\star$ is a term that can be induced by symmetry, $\beta \in]0,1[$ is a design parameter, $Q \in \mathbb{R}^{n \times n_y}$, and $P = P^T \succ 0$ is a symmetric positive definite matrix.

Nominal Gain Design (Nom-G): For the nominal form of the linear system (2), i.e., in the absence of disturbances and noises, the observer gain L can be designed as [71, eq. (36)]

$$L = P^{-1}Y,$$

where $P = P^T \succ 0$ is a symmetric positive definite matrix and $Y \in \mathbb{R}^{n \times n_y}$ has to fulfill

$$\begin{bmatrix} \mu P & \star \\ PA - YC & P \end{bmatrix} \succ 0$$

for a scalar $\mu \in]0, 1]$. The observer gain is stable with a decay rate μ for the nominal form of the system.

3.3 Interval Observer

We only consider one approach to design the observer gain L in Alg. 1.

H-infinity-based design (Hinf-G): A H-infinity-based optimization problem to find L is devised in [65, eq. 16]:

$$\min_{\gamma} \ \gamma^2$$

subject to

$$\begin{bmatrix} I - P & \star & \star & \star \\ 0 & -\gamma^2 I & \star & \star \\ 0 & 0 & -\gamma^2 I & \star \\ PA - YC & PE & -YF & -P \end{bmatrix} \prec 0,$$

where $Y = PL$, $\gamma > 0$ is a scalar, and $P = P^T \succ 0$ is a symmetric positive definite matrix. The observer gain is thus computed such that the estimation error is robust against disturbances and noise influences.

3.4 Summary

The design of the observer gain L is computed at each step using the FRad-C technique, while for PRad-E, Nom-G, and Hinf-G, the gain L is pre-computed off-line. Considering all the zonotopic state observers discussed earlier, the order of the zonotopic estimation set $\mathcal{S}_k$ increases with k irrespective of the design approach. To circumvent this problem, several zonotope order-reduction techniques [3, 19, 26, 31, 33, 76] have been proposed to bound the higher-order zonotope by a lower-order one, where [33] proposed the first approach and [19] first reduced zonotopes by sorting generators. These methods are analyzed in our subsequent performance evaluation.

4 Performance Evaluation

In this section, we evaluate the performance of the presented zonotopic observers and compare them with the following observers using ellipsoids and constrained zonotopes:

(1) A strip-based observer with optimal bounding ellipsoids (ESO-A), where the intersection with the measurement set is performed according to [28] and the prediction step according to [42]. When using the prediction approach in [28], the results would have been too over-approximative.
(2) A strip-based observer with selective observation update for linear-disturbed systems (ESO-B) [42].
(3) An ellipsoidal set-propagation observer using ellipsoidal invariant sets for error estimation (ESO-C) [44].
(4) A robust H-infinity-based ellipsoidal interval observer (ESO-D) [45].
(5) A constrained zonotopic observer with direct intersection (CZN-A) [62].
(6) A constrained zonotopic observer with strip-based intersection optimized using F-radius minimization (CZN-B) [2].

All ellipsoids (initial set, disturbance set, and sensor noise set) are chosen so that they are enclosed in the corresponding zonotopes. We evaluated all observers on an Intel(R) Core(TM) i7-8565U CPU @ 1.80GHz machine with MATLAB 2020b with single thread executions [4]. For all set operations we have used the CORA toolbox [4] and optimization problems have been solved using the YALMIP toolbox [43] with the Mosek solver [9].

4.1 Performance metrics

We evaluate all observers with respect to tightness of the estimated sets and computation time. The relative rms (root-mean-square) values of the interval radius $r_{i,k,l}$ of the i^{th} state variable at step k out of N_s time steps of observer l are computed as:

$$v_{i,l} = \frac{\tilde{r}_{i,l}}{\min(\tilde{r}_{i,1}, \ldots, \tilde{r}_{i,n_l})}, \ \tilde{r}_{i,l} = \sqrt{\left(\frac{1}{N_s} \sum_{k=0}^{N_s - 1} r_{i,k,l}^2 \right)}. \tag{9}$$

We are not using volume as a metric due to its computational complexity for zonotopes (see [1, Sec. 6.2]); also, volume approximation methods for zonotopes are not yet accurate enough.

4.2 Case Study

We consider the case study of estimating states of an autonomous vehicle. Typically, the yaw rate and the longitudinal velocity of the vehicle are measurable [68]. Using these measurements, the lateral acceleration of the vehicle can also be computed. However, the lateral velocity

[4] The implementation files for all set-based observers discussed in this paper and further results are provided at https://MatthiasAlthoff@bitbucket.org/MatthiasAlthoff/set-based-observer-comparison-lti-2021.git

or side slip are difficult to measure [63,68], which are important values for safe motion planning of autonomous vehicles. Due to the safety-criticality of autonomous vehicles, it is essential that we reconstruct the set of possible states instead of a single estimate.

We use the vehicle model in [7] and combine it with the steer column dynamics in [63] to obtain an Euler-discretized model in the form of (2) for a sampling time of $T_s = 10$ milliseconds (ms). The system states are $x_{v6} = [\tilde{\beta},\ \dot{\Psi},\ \Psi,\ s_y,\ \delta,\ \dot{\delta}]^T$, where $\tilde{\beta}, \Psi$ are the side slip and yaw angles in radian, s_y is the lateral displacement in m, $\dot{\Psi}$ is the yaw rate in radian/s, δ is the steer angle in radian and $\dot{\delta}$ is the steer rate in radian/s. The initial state is chosen as the origin, the control output u_k is the steering torque from the motor of the electronic power steering unit, and the measurements y_k are the lateral acceleration a_y, steering angle δ, and vehicle lateral position s_y from the lane center line [53]. For space reasons, the system equations and the set of disturbances and sensor noises can only be found online [4].

We consider a double-lane change maneuver executed at a fixed longitudinal velocity of 15 m/s. To analyze the scalability of various set-based observers, we also consider reduced-order vehicle systems with the respective state vectors $x_{v4} = [\tilde{\beta},\ \dot{\Psi},\ \Psi,\ s_y]^T$ and $x_{v2} = [\tilde{\beta},\ \dot{\Psi}]^T$. For all these vehicular systems, the side slip angle is not measurable and thus estimated. It was observed that the performance of most observers showed no significant variations with respect to the dimension of the vehicular system so that we only present the results of the full system. The results of the other models are provided online [4].

4.3 Results

The performance metrics from Sec. 4.1 are listed in Tab. 3, where t_{comp} is the computation time per iteration in milliseconds (ms). Since VolMin-A has extremely high computational costs, we could only apply it to the smallest vehicle model and thus it is missing in Tab. 3. As examples, we visualize the estimated intervals of all states using the FRad-A observer in Fig. 2, the FRad-C observer in Fig. 3, and the Hinf-G observer in Fig. 4.

We have also analyzed the effect of using different order reduction techniques. Overall, order reduction has only a limited effect (i.e., less than 18 % change in interval radii of measured states). Due to the limited influence on the best observers we only present these results online [4].

Zonotopes or Constrained Zonotopes or Ellipsoids?

- *Tightness*: Since constrained zonotopes are closed under linear maps, Minkowski sum, and intersection, they provide the tightest results as shown in Tab. 3. However, one cannot directly compute their intervals for a given variable since this requires solving linear programs [62, eq. (25),(26)], which cannot be solved in real time for the considered problem. In contrast, intervals of zonotopes and ellipsoids can be easily obtained. The estimated interval radii of zonotopic observers are significantly tighter than those of ellipsoidal observers, irrespective of the used method; see Tab. 3. The worst zonotopic strip-based observer PRad-A has a better accuracy than the best ellipsoidal strip-based observer ESO-A. Likewise, the worst zonotopic set-propagation observer Nom-G is more accurate than the best ellipsoidal set-propagation observer ESO-C.
- *Computational efficiency*: The computational costs of ellipsoidal observers are roughly an order of magnitude lower for set-propagation techniques compared to zonotopic observers in Tab. 3. However, for strip-based techniques, the computation times are more similar. Constrained zonotopes have a larger computation time compared to the other set representations, except for VolMin-B. This time is significantly enlarged by 492 ms per time step when the interval of values for a specific variable is required (zonotopes: 0.1 ms. ellipsoids: 6.6 ms).

Strip-Based or Set-Propagation or Interval Observer?

- *Tightness*: Except PRad-A, all zonotopic strip-based observers have an average relative radius below 4 in Tab. 3, while no zonotopic set-propagation observer has an average relative score below 4.
- *Computational efficiency*: The fastest computational times have been obtained for set-propagation observers when using ellipsoids. However, also when using zonotopes, set-propagation observers are slightly faster compared to the other observer types as shown in Tab. 3. All approaches have similar computational costs and are real-time capable ($t_{cp} < 10$ ms; step size is 10 ms), except VolMin-B. Obviously, the computational time of observers requiring real-time updates of design parameters, i.e., FRad-A, FRad-B, FRad-C, ESO-A, and ESO-B are slightly higher than the P-radius techniques, where the design gains are pre-computed.
- *Ratio of tightness compared to computational efficiency*: A particularly good ratio of tightness compared to computational efficiency has been obtained by PRad-B and PRad-C-II in our use case.

5 Conclusions

Irrespective of the design approach, zonotopic observers outperform ellipsoidal observers in terms of tightness.

Table 3
Relative rms values v_i according to (9). Indices of unmeasured states: $1, 3, 6$. Indices of measured states: $2, 4, 5$ ($\dot{\psi} = a_y/v$).

Technique	**Set representation**	**Ready for control**	v_1	v_2	v_3	v_4	v_5	v_6	$\mathbf{t_{comp}}$ **in [ms]**
strip-based observers									
VolMin-B	zonotope	✗	4.129	1.000	1.636	1.055	7.136	1.286	131.2
FRad-A	zonotope	✗	1.854	1.357	2.893	2.619	2.862	1.584	0.546
FRad-B	zonotope	✗	2.297	1.189	2.878	2.147	2.868	3.124	0.375
PRad-A	zonotope	✗	8.321	214.8	6.240	21.39	6.154	6.537	0.444
PRad-B	zonotope	✗	2.583	1.354	1.750	1.464	1.865	4.317	0.252
PRad-C-I	zonotope	✗	3.239	1.560	6.417	3.438	5.019	3.687	0.259
PRad-C-II	zonotope	✗	2.460	1.237	1.639	1.064	1.234	4.938	0.268
PRad-D	zonotope	✗	2.433	1.002	1.641	1.069	1.247	6.539	0.279
CZN-A	constr. zono.	✗	1.010	1.000	1.000	1.000	1.016	1.009	3.412
CZN-B	constr. zono.	✗	1.000	1.000	1.043	1.003	1.000	1.000	3.245
ESO-A	ellipsoid	✗	3.211	292.8	29.39	94.33	6.554	3.502	1.090
ESO-B	ellipsoid	✗	4.232	486.0	35.83	177.5	9.418	5.430	1.911
set-propagation observers									
FRad-C	zonotope	✓	2.022	32.35	3.315	3.605	3.378	1.926	0.471
PRad-E	zonotope	✓	2.640	32.03	2.552	2.670	3.166	4.379	0.304
Nom-G	zonotope	✓	2.702	32.79	2.374	2.293	3.199	4.839	0.258
ESO-C	ellipsoid	✓	1.995	65.90	7.554	4.811	5.184	4.463	0.052
ESO-D	ellipsoid	✓	10.83	372.5	42.82	27.25	29.28	25.92	0.051
interval observer									
Hinf-G	zonotope	✓	2.669	37.26	3.456	3.298	3.929	3.522	0.251
smallest absolute radii									
			0.139	0.006	0.061	0.094	0.082	3.236	

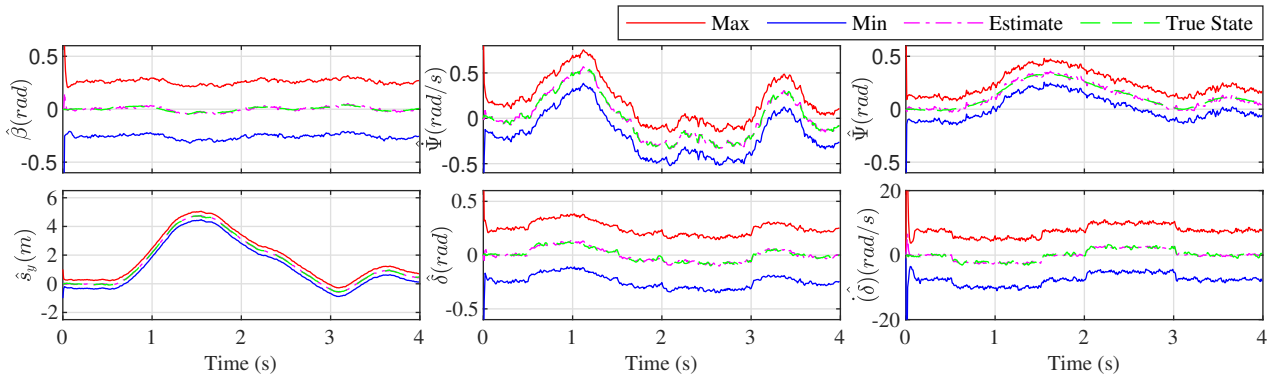

Fig. 2. Estimated interval centers and bounds for all states using the FRad-A technique.

While constrained zonotopic observers are even tighter, computing the intervals of state variables requires solving linear programs, rendering them only practical when explicit bounds for state variables are not required. Regarding computational costs, ellipsoidal observers have significantly lower computational costs than zonotopic observers when using set-propagation designs. All presented observers, except those based on volume minimization, can be implemented in real-time for the considered automotive systems. We also observed that zonotope reduction techniques had only a minor impact on the overall performance. A particularly good ratio of tightness compared to computational efficiency has been obtained by PRad-B and PRad-C-II in our use case. Due to the recent progress, more real-world applications would be commendable. When the application does not accept delays in the result of guaranteed bounds, set propagation techniques should be used. If the application requires explicit bounds for individual state variables, zonotopes should be selected. Finally,

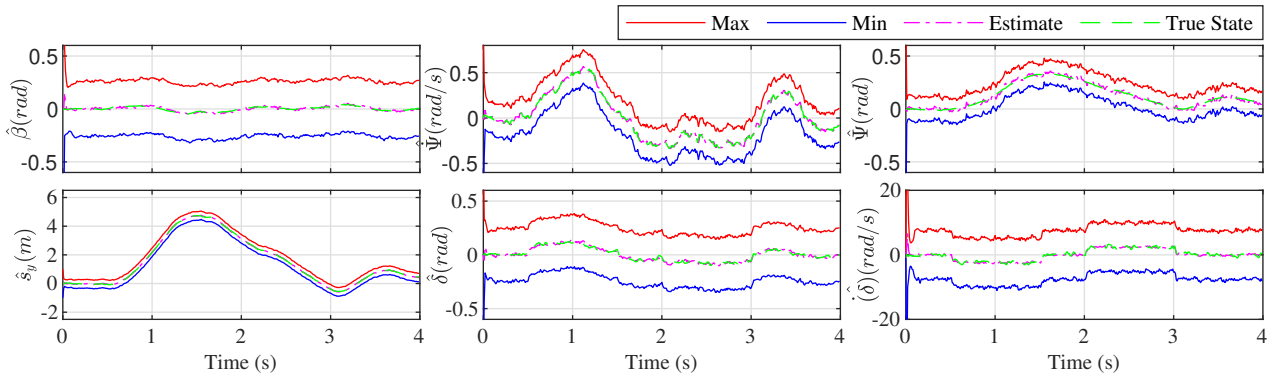

Fig. 3. Estimated interval centers and bounds for all states using the FRad-C technique.

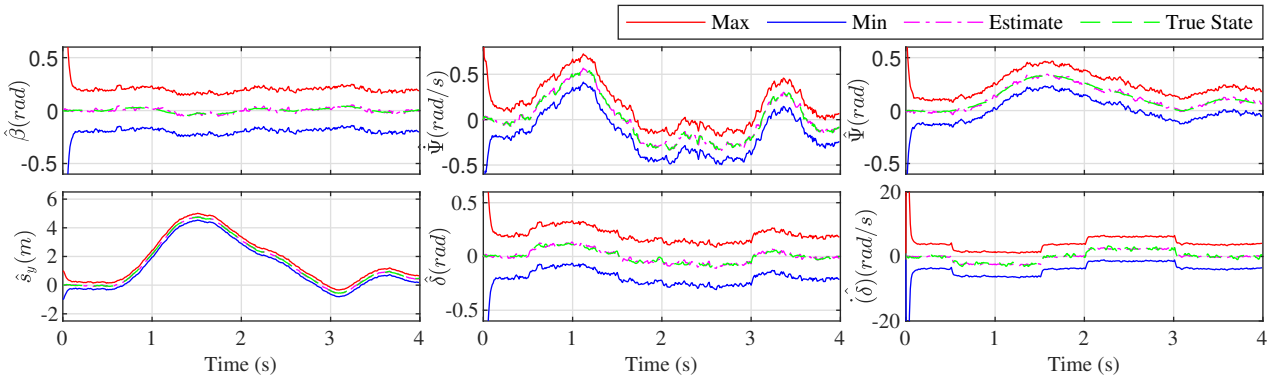

Fig. 4. Estimated interval centers and bounds for all states using the Hinf-G technique.

we would like to stress that we only focused on linear time-invariant systems. For linear time-varying systems and nonlinear systems, the performance of certain concepts might shift substantially.

Acknowledgements

The authors gratefully acknowledge the partial financial support of this work by the European Research Council (ERC) project justITSELF under grant agreement No 817629 and the Ford Motor Company.

References

[1] T. Alamo, J. M. Bravo, and E. F. Camacho. Guaranteed state estimation by zonotopes. *Automatica*, 41(6):1035–1043, 2005.

[2] A. Alanwar, V. Gassmann, X. He, H. Said, H. Sandberg, K. H. Johansson, and M. Althoff. Privacy preserving set-based estimation using partially homomorphic encryption. arXiv:2010.11097.

[3] M. Althoff. *Reachability Analysis and its Application to the Safety Assessment of Autonomous Cars*. Dissertation, Technische Universität München, 2010. http://nbn-resolving.de/urn/resolver.pl?urn:nbn:de:bvb:91-diss-20100715-963752-1-4.

[4] M. Althoff. An introduction to CORA 2015. In *Proc. of the Workshop on Applied Verification for Continuous and Hybrid Systems*, pages 120–151, 2015.

[5] M. Althoff and J. M. Dolan. Online verification of automated road vehicles using reachability analysis. *IEEE Transactions on Robotics*, 30(4):903–918, 2014.

[6] M. Althoff and G. Frehse. Combining zonotopes and support functions for efficient reachability analysis of linear systems. In *Proc. of the 55th IEEE Conference on Decision and Control*, pages 7439–7446, 2016.

[7] M. Althoff, M. Koschi, and S. Manzinger. CommonRoad: Composable benchmarks for motion planning on roads. In *Proc. of the IEEE Intelligent Vehicles Symposium*, pages 719–726, 2017.

[8] M. Althoff, O. Stursberg, and M. Buss. Reachability analysis of nonlinear systems with uncertain parameters using conservative linearization. In *Proc. of the 47th IEEE Conference on Decision and Control*, pages 4042–4048, 2008.

[9] MOSEK ApS. The MOSEK optimization toolbox for MATLAB manual. version 7.1 (revision 28)., 2015.

[10] D. P. Bertsekas and I. B. Rhodes. Recursive state estimation for a set-membership description of uncertainty. *IEEE Transactions on Automatic Control*, 16:117–128, 1971.

[11] F. Blanchini and S. Miani. *Set-Theoretic Methods in Control*. Birkhäuser Boston, 2008.

[12] J. Blesa, V. Puig, J. Romera, and J. Saludes. Fault diagnosis of wind turbines using a set-membership approach. *IFAC Proceedings Volumes*, 44(1):8316–8321, 2011.

[13] J. Blesa, D. Rotondo, V. Puig, and F. Nejjari. FDI and FTC of wind turbines using the interval observer approach

and virtual actuators/sensors. *Control Engineering Practice*, 24:138–155, 2014.

[14] S. Bogomolov, M. Forets, G. Frehse, F. Viry, A. Podelski, and C. Schilling. Reach set approximation through decomposition with low-dimensional sets and high-dimensional matrices. In *Proc. of the 21st International Conference on Hybrid Systems: Computation and Control*, pages 41–50, 2018.

[15] J. M. Bravo, T. Alamo, and E. F. Camacho. Bounded error identification of systems with time-varying parameters. *IEEE Transactions on Automatic Control*, 51(7):1144–1150, 2006.

[16] D. D. Bremner. On the complexity of vertex and facet enumeration for convex polytopes, 1997. McGill University.

[17] S. Ben Chabane. *Fault detection techniques based on set-membership state estimation for uncertain systems*. Dissertation, Université Paris-Saclay, 2015.

[18] L. Chisci, A. Garulli, and G. Zappa. Recursive state bounding by parallelotopes. *Automatica*, 32(7):1049–1055, 1996.

[19] C. Combastel. A state bounding observer based on zonotopes. In *Proc. of the European Control Conference*, pages 2589–2594, 2003.

[20] C. Combastel. A state bounding observer for uncertain non-linear continuous-time systems based on zonotopes. In *Proc. of the 44th IEEE Conference on Decision and Control, and the European Control Conference*, pages 7228–7234, 2005.

[21] C. Combastel. Merging Kalman filtering and zonotopic state bounding for robust fault detection under noisy environment. *IFAC-PapersOnLine*, 48(21):289–295, 2015.

[22] C. Combastel. Zonotopes and Kalman observers: Gain optimality under distinct uncertainty paradigms and robust convergence. *Automatica*, 55:265–273, 2015.

[23] C. Durieu, É. Walter, and B. Polyak. Multi-input multi-output ellipsoidal state bounding. *Journal of Optimization Theory and Applications*, 111(2):273–303, 2001.

[24] D. Efimov, T. Raïssi, S. Chebotarev, and A. Zolghadri. Interval state observer for nonlinear time varying systems. *Automatica*, 49(1):200–205, 2013.

[25] P. Falcone, M. Ali, and J. Sjöberg. Predictive threat assessment via reachability analysis and set invariance theory. *IEEE Transactions on Intelligent Transportation Systems*, 12(4):1352–1361, 2011.

[26] A. Girard. Reachability of uncertain linear systems using zonotopes. In *Hybrid Systems: Computation and Control*, LNCS 3414, pages 291–305. Springer, 2005.

[27] A. Girard, C. Le Guernic, and O. Maler. Efficient computation of reachable sets of linear time-invariant systems with inputs. In *Hybrid Systems: Computation and Control*, LNCS 3927, pages 257–271. Springer, 2006.

[28] S. Gollamudi, S. Nagaraj, S. Kapoor, and Y. F. Huang. Set-membership state estimation with optimal bounding ellipsoids. In *Proc. of the International Symposium on Information Theory and its Applications*, pages 262–265, 1996.

[29] J. L. Gouzé, A. Rapaport, and M. Z. Hadj-Sadok. Interval observers for uncertain biological systems. *Ecological Modelling*, 133(1):45–56, 2000.

[30] N. Kochdumper, A. Tarraf, M. Rechmal, M. Olbrich, L. Hedrich, and M. Althoff. Establishing reachset conformance for the formal analysis of analog circuits. In *Proc. of the 25th Asia and South Pacific Design Automation Conference*, pages 199–204, 2020.

[31] A.-K. Kopetzki, B. Schürmann, and M. Althoff. Methods for order reduction of zonotopes. In *Proc. of the 56th IEEE Conference on Decision and Control*, pages 5626–5633, 2017.

[32] E. K. Kostousova. State estimation for dynamic systems via parallelotopes optimization and parallel computations. *Optimization Methods and Software*, 9(4):269–306, 1998.

[33] W. Kühn. Rigorously computed orbits of dynamical systems without the wrapping effect. *Computing*, 61:47–67, 1998.

[34] A. A. Kurzhanskiy and P. Varaiya. Ellipsoidal toolbox. Technical Report UCB/EECS-2006-46, EECS Department, University of California, Berkeley, 2006.

[35] V. T. H. Le, T. Alamo, E. F. Camacho, C. Stoica, and D. Dumur. A new approach for guaranteed state estimation by zonotopes. pages 9242–9247, 2011.

[36] V. T. H. Le, T. Alamo, E. F. Camacho, C. Stoica, and D. Dumur. Zonotopic set-membership estimation for interval dynamic systems. In *Proc. of the IEEE American Control Conference*, pages 6787–6792, 2012.

[37] V. T. H. Le, C. Stoica, T. Alamo, E. F. Camacho, and D. Dumur. Zonotope-based set-membership estimation for multi-output uncertain systems. In *Proc. of the IEEE International Symposium on Intelligent Control*, pages 212–217, 2013.

[38] V. T. H. Le, C. Stoica, T. Alamo, E. F. Camacho, and D. Dumur. Zonotopic guaranteed state estimation for uncertain systems. *Automatica*, 49(11):3418–3424, 2013.

[39] V. T. H. Le, C. Stoica, D. Dumur, T. Alamo, and E. F. Camacho. Robust tube-based constrained predictive control via zonotopic set-membership estimation. In *Proc. of the IEEE Conference on Decision and Control and European Control Conference*, pages 4580–4585, 2011.

[40] D. Limon, I. Alvarado, T. Alamo, and E. F.Camacho. Robust tube-based MPC for tracking of constrained linear systems with additive disturbances. *Journal of Process Control*, 20(3):248–260, 2010.

[41] S. B. Liu and M. Althoff. Reachset conformance of forward dynamic models for the formal analysis of robots. In *Proc. of the IEEE/RSJ International Conference on Intelligent Robots and Systems*, pages 370–376, 2018.

[42] Y. Liu, Y. Zhao, and F. Wu. Ellipsoidal state-bounding-based set-membership estimation for linear system with unknown-but-bounded disturbances. *IET Control Theory & Applications*, 10(4):431–442, 2016.

[43] J. Lofberg. YALMIP : a toolbox for modeling and optimization in MATLAB. In *Proc. of the IEEE International Conference on Robotics and Automation*, pages 284–289.

[44] N. Loukkas, J. J. Martinez, and N. Meslem. Set-membership observer design based on ellipsoidal invariant sets. *IFAC-PapersOnLine*, 50(1):6471–6476, 2017.

[45] J. J. Martinez, N. Loukkas, and N. Meslem. H_∞ set-membership observer design for discrete-time LPV systems. *International Journal of Control*, 93(10):2314–2325, 2020.

[46] F. Mazenc and O. Bernard. Interval observers for linear time-invariant systems with disturbances. *Automatica*, 47(1):140–147, 2011.

[47] S. Mitra, T. Wongpiromsarn, and R. M. Murray. Verifying cyber-physical interactions in safety-critical systems. *IEEE Security and Privacy*, 11(4):28–37, 2013.

[48] B. T. Polyak, S. A. Nazin, C. Durieu, and E. Walter. Ellipsoidal parameter or state estimation under model uncertainty. *Automatica*, 40(7):1171–1179, 2004.

[49] M. Pourasghar, V. Puig, and C. Ocampo-Martinez. Comparison of set-membership and interval observer approaches for state estimation of uncertain systems. In *Proc. of the IEEE European Control Conference*, pages 1111–1116, 2016.

[50] M. Pourasghar, V. Puig, and C. Ocampo-Martinez. Interval observer versus set-membership approaches for fault detection in uncertain systems using zonotopes. *International Journal of Robust and Nonlinear Control*, 29(10):2819–2843, 2019.

[51] V. Puig. Fault diagnosis and fault tolerant control using set-membership approaches: Application to real case studies. *International Journal of Applied Mathematics and Computer Science*, 20:619–635, 2010.

[52] V. Puig, P. Cuguero, and J. Quevedo. Worst-case state estimation and simulation of uncertain discrete-time systems using zonotopes. In *Proc. of the IEEE European Control Conference*, pages 1691–1697, 2001.

[53] R. Rajamani, H.-S. Tan, B. K. Law, and W.-B. Zhang. Demonstration of integrated longitudinal and lateral control for the operation of automated vehicles in platoons. *IEEE Transactions on Control Systems Technology*, 8(4):695–708, 2000.

[54] R. Rajkumar, I. Lee, L. Sha, and J. Stankovic. Cyber-physical systems: The next computing revolution. In *Proc. of the 47th Design Automation Conference*, pages 731–736, 2010.

[55] T. Raïssi and D. Efimov. Some recent results on the design and implementation of interval observers for uncertain systems. *Automatisierungstechnik*, 66(3):213–224, 2018.

[56] B. S. Rego, G. V. Raffo, J. K. Scott, and D. M. Raimondo. Guaranteed methods based on constrained zonotopes for set-valued state estimation of nonlinear discrete-time systems. *Automatica*, 111, 2020. article no. 108614.

[57] B. S. Rego, D. M. Raimondo, and G. V. Raffo. Path tracking control with state estimation based on constrained zonotopes for aerial load transportation. In *Proc. of the 57th IEEE Conference on Decision and Control*, pages 1979–1984, 2018.

[58] H. Roehm, J. Oehlerking, M. Woehrle, and M. Althoff. Reachset conformance testing of hybrid automata. In *Proc. of Hybrid Systems: Computation and Control*, pages 277–286, 2016.

[59] H. Roehm, J. Oehlerking, M. Woehrle, and M. Althoff. Model conformance for cyber-physical systems: A survey. *ACM Transactions on Cyber-Physical Systems*, 3(3):Article 30, 2019.

[60] B. Schürmann, N. Kochdumper, and M. Althoff. Reachset model predictive control for disturbed nonlinear systems. In *Proc. of the 57th IEEE Conference on Decision and Control*, pages 3463–3470, 2018.

[61] F. Schweppe. Recursive state estimation: Unknown but bounded errors and system inputs. *IEEE Transactions on Automatic Control*, 13(1):22–28, 1968.

[62] J. K. Scott, D. M. Raimondo, G. R. Marseglia, and R. D. Braatz. Constrained zonotopes: A new tool for set-based estimation and fault detection. *Automatica*, 69:126–136, 2016.

[63] B. Soualmi, C. Sentouh, J. C. Popieul, and S. Debernard. Automation-driver cooperative driving in presence of undetected obstacles. *Control Engineering Practice*, 24:106–119, 2014.

[64] W. Tang, Z. Wang, Y. Shen, M. Rodrigues, and D. Theilliol. Fault detection based on multi-objective observer and interval hull computation. *IFAC-PapersOnLine*, 51(24):332–337, 2018.

[65] W. Tang, Z. Wang, Y. Wang, T. Raïssi, and Y. Shen. Interval estimation methods for discrete-time linear time-invariant systems. *IEEE Transactions on Automatic Control*, 64(11):4717–4724, 2019.

[66] H. Wang, I. V. Kolmanovsky, and J. Sun. Zonotope-based recursive estimation of the feasible solution set for linear static systems with additive and multiplicative uncertainties. *Automatica*, 95:236–245, 2018.

[67] Y. Wang, T. Alamo, V. Puig, and G. Cembrano. A distributed set-membership approach based on zonotopes for interconnected systems. In *Proc. of the IEEE Conference on Decision and Control*, pages 668–673, 2018.

[68] Y. Wang, D. M. Bevly, and R. Rajamani. Interval observer design for LPV systems with parametric uncertainty. *Automatica*, 60:79–85, 2015.

[69] Y. Wang and V. Puig. Zonotopic extended Kalman filter and fault detection of discrete-time nonlinear systems applied to a quadrotor helicopter. In *Proc. of the 3rd IEEE Conference on Control and Fault-Tolerant Systems*, pages 367–372, 2016.

[70] Y. Wang, V. Puig, and G. Cembrano. Robust fault estimation based on zonotopic Kalman filter for discrete-time descriptor systems. *International Journal of Robust and Nonlinear Control*, 28(16):5071–5086, 2018.

[71] Y. Wang, V. Puig, and G. Cembrano. Set-membership approach and Kalman observer based on zonotopes for discrete-time descriptor systems. *Automatica*, 93:435–443, 2018.

[72] Y. Wang, Z. Wang, V. Puig, and G. Cembrano. Zonotopic set-membership state estimation for discrete-time descriptor LPV systems. *IEEE Transactions on Automatic Control*, 64(5):2092–2099, 2019.

[73] Y. Wang, M. Zhou, V. Puig, G. Cembrano, and Z. Wang. Zonotopic fault detection observer with $\mathcal{H}_-$ performance. In *Proc. of the 36th IEEE Chinese Control Conference*, pages 7230–7235, 2017.

[74] K. Witheephanich, L. Orihuela, R. A. Garcia, and J. M. Escano. Min-max model predictive control with robust zonotope-based observer. In *Proc. of the UKACC 11th IEEE International Conference on Control*, pages 1–6, 2016.

[75] J. Xiong. *Set-membership state estimation and application on fault detection.* Dissertation, Automatique / Robotique. Institut National Polytechnique de Toulouse - INPT, 2013.

[76] X. Yang and J. K. Scott. A comparison of zonotope order reduction techniques. *Automatica*, 95:378–384, 2018.

[77] G. Zheng, D. Efimov, and W. Perruquetti. Design of interval observer for a class of uncertain unobservable nonlinear systems. *Automatica*, 63:167–174, 2016.